

# Preparation and Characterization of porous Carbon/Nickel Nanofibers for Supercapacitor

Dawei Gao<sup>1,2</sup>, Lili Wang<sup>1</sup>, Xin Xia<sup>2</sup>, Hui Qiao<sup>2</sup>, Yibing Cai<sup>2</sup>,  
Fenglin Huang<sup>2</sup>, Kishor Gupta<sup>3</sup>, Qufu Wei<sup>2</sup>, Satish Kumar<sup>3</sup>

<sup>1</sup>College of Textiles and Clothing, Yangcheng Institute of Technology, Yangcheng, Jiangsu, CHINA

<sup>2</sup>Key Laboratory of Eco-textiles, Ministry of Education, Jiangnan University, Wuxi, Jiangsu, CHINA

<sup>3</sup>School of Materials Science and Engineering, Georgia Institute of Technology, Atlanta, GA USA

Correspondence to:

Qufu Wei email: [qfwei@jiangnan.edu.cn](mailto:qfwei@jiangnan.edu.cn)

## ABSTRACT

Two polymer solutions of polyacrylonitrile, polyvinyl pyrrolidone, and  $\text{Ni}(\text{CH}_3\text{COOH})_2$  in dimethylformamide were electrospun into ternary composite nanofibers, followed by stabilization and carbonization processes to obtain porous carbon/nickel composite nanofibers with diameters of 100-200 nm. The study revealed that carbon/nickel composite nanofibers were successfully prepared, which allowed nickel particles with diameters of 20-70 nm to be uniformly distributed in the carbon nanofibers. It was also observed that the fibrous structures with particles embedded formed and the fibers broke into shorter fibers after sintering. X-ray diffraction indicated that embedded particles crystallized with the face centered cubic structure. The Brunauer-Emmett-Teller analysis revealed that carbon/nickel composite nanofibers with meso-pores possessed larger specific surface area than that of carbon nanofibers. The specific capacitance of the composite nanofiber electrode was as high as 103.8 F/g and showed stable cyclicality (73.8%).

## INTRODUCTION

Over the past few decades, the development of carbon materials of various forms with unique structures and properties has attracted considerable attention because of their potential applications in supercapacitors [1-4]. Traditional activated porous carbon fibers are obtained mainly by chemical activation with KOH [5, 6] or NaOH [7] and physical activation with steam [8, 9] and carbon dioxide [10]. A simple, yet effective and economical technique for creating porous carbon with both large surface area and incorporated functional component is needed.

One-dimensional porous carbon fibers [11, 12], and carbon/metal composite fibers [13, 14], with well-controlled pore structures and well-dispersed nanometer scale metallic compounds, are desired for many practical applications. However, only a few studies have covered the carbon/nickel (C/Ni) composites prepared by the method of using electrospinning electrode materials for supercapacitors [15]. Here, we report an easy method to obtain porous carbon/nickel nanofibers with uniform and controllable pore sizes by electrospinning and subsequent carbonization processes, in which two polymer solutions polyacrylonitrile and polyvinyl pyrrolidone (PAN and PVP) and  $\text{Ni}(\text{CH}_3\text{COOH})_2$  ( $\text{Ni}(\text{OAc})_2$ ) were used as C/Ni composite nanofiber precursors because the PVP phase decomposed during thermal treatment. The porous carbon nanofibers were obtained afterwards. The nickel particles were uniformly incorporated into the porous carbon fibers, which would enhance not only the conductivity of the fiber mat but also the electron transfer between nickel particles and the carbon substrate. The electrochemical behavior and cycling performance of the C/Ni composite nanofibers were also discussed.

## EXPERIMENTAL

### Fibers preparation

Electrospinning is now a versatile and effective method for fabricating functional nanofibers, which are exceptionally long and uniform in diameter ranging from tens of nanometers to several micrometers [16]. The preparation of the composite nanofibers was reported in our previous work [17]. In

short, the N,N-dimethylformamide (DMF) solutions of PAN/PVP (7:3, 10wt %) containing 50wt% Ni(OAc)<sub>2</sub> were prepared at room temperature, in which the DMF was used as received and the molecular weights of PAN and PVP were 79,100 and 40,000, respectively. For comparison of the effect of different nickel content on conductivity, solutions of PAN and PAN/PVP containing 10wt% and 30wt% Ni(OAc)<sub>2</sub> were also prepared. The positive voltage, working distance, and flow rate were 15 kV, 15 cm, and 0.4 mL/h, respectively. The collected electrospun PAN/PVP/Ni(OAc)<sub>2</sub> precursor nanofibers were dried and then stabilized in an air environment at 250 °C for 4 h (heating rate at 2 °C min<sup>-1</sup>) and then carbonized at 800 °C for 6 h in argon atmosphere (heating rate at 5 °C min<sup>-1</sup>) to obtain the resultant composite carbon nanofibers.

### **Structural Characterization**

The wide-angle X-ray diffraction (XRD) patterns of the materials were obtained using a Rigaku RU-H3R (Rigaku, Tokyo, Japan) equipped with an image plate. Scanning electron microscopy (FE-SEM, JSM-5600) was used to observe the structures and surface morphology of nanofibers. The inner structure of the nanofiber was examined using a transmission electron microscope (TEM, Philips, and CM120). The samples for TEM were prepared by dispersing the composite fibers in ethanol; and the dispersion was then dropped on carbon-copper grids. Surface area of CNFs was measured using Brunauer-Emmett-Teller (BET) nitrogen adsorption method (Micromeritics Gemini 2360).

### **Electrochemical Performance**

The electrochemical properties of 50wt% Ni(OAc)<sub>2</sub> precursor were detected on Solartron 1470 cell test station (Solartron Analytical, Houston, TX). In the galvanostatic measurements, the cell was charged and discharged from 0 to 0.8 V in 6 M KOH aqueous electrolyte at constant current densities of 0.5, 2.5, 5.0, 15.0, 25.0 A/g. In CV measurements, scan rates of 1, 5, 10, 50 and 100 mVs<sup>-1</sup> were used. Nickel current collector was used in this two electrode test cell. The electrodes were 0.25 inch diameter. The specific capacitance was reported at 0.1 V of discharging curve for all the samples.

## **RESULTS AND DISCUSSION**

### **Crystal Structures**

Figure 1 shows 1D integrated X-ray diffraction intensity profile of the C/Ni composite nanofibers annealed at 800 °C, which was extracted from its 2D wide angle X-ray image shown in the inset of Fig. 1. The broad peaks near 25° corresponded to the (002) diffraction peaks of graphite (JCPDS-ICDD 75-1261), suggesting that the PAN fiber was converted into disordered carbon. The other two peaks near 44.42°, 51.78°, which corresponded to (220) and (200) crystal planes, were well indexed to face centered cubic nickel phase (JCPDS-ICDD 65-2856). Since nickel acetate decomposed at a temperature of around 200 °C [17, 18], nickel oxide could be obtained in the composite when the preoxidation was carried out at 230 °C. As the temperature further increased in the annealing process, PAN decomposed gradually into carbon. This could also reduce the nickel oxide into metal at the high temperature. Thus, the final product was a carbon-nickel composite. Assuming the complete conversion of nickel oxide into metallic nickel and a fully dense morphology of the fibers, the composition of the C/Ni composite was about C (50 wt.%)–Ni (50 wt.%). The lattice parameters a, b, and c calculated from the XRD spectrum for the nickel nanocrystals were a=b=c=0.3524 nm. The strongest and most predominate peak at 2θ=44.42° was representative of the (220) phase reflections. Therefore, the average crystallite sizes along the (220) plane were measured using the Scherrer formula shown in the following equation (1):

$$L = 0.9\lambda/\beta\cos\theta \quad (1)$$

where  $\lambda$  is the wavelength of the X-ray radiation (Cu K $\alpha$ ,  $\lambda=0.15418$  nm),  $\theta$  is the diffraction angle of the (220) peak and  $\beta$  is defined as the full width at half maximum. By applying this equation to peak (220), the original crystal size of nickel particles was found to be ca. 15 nm. It was much smaller than the diameter of carbon fibers, indicating that the nickel particles could be easily dispersed in the fibers.

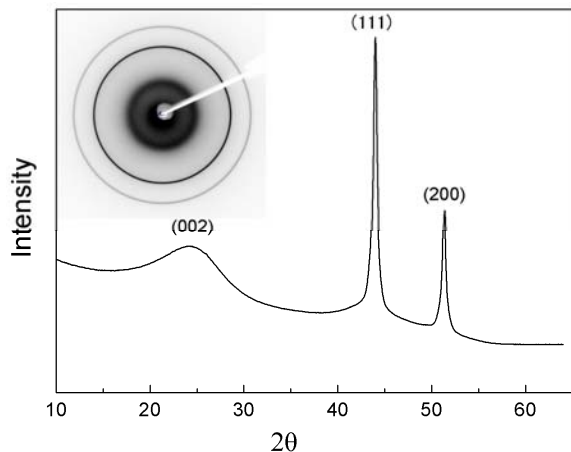


FIGURE 1. XRD pattern of the C/Ni composite nanofibers annealed at 800 °C. Inset: 2D X-ray image for the same sample.

### **Morphology Observation**

The SEM images of PAN/PVP/Ni(OAc)<sub>2</sub> precursor and carbonized composite nanofibers are shown in *Figure 2*. The PAN/PVP/Ni(OAc)<sub>2</sub> precursor nanofibers exhibited fibrous structure and relatively smooth surface morphology with uniform diameter of

ca. 200 nm, as presented in *Figure 2(a)*. The TEM images revealed that shorter fibers embedded with Ni particles were formed during the high-temperature carbonization process indicating low breaking strength of the fiber (*Figure 2(b)*). The formation of metallic Ni was caused by the reducing environment created by the carbonization reactions. From the (TEM) image illustrated in *Figure 2(c)*, it was also clear that Cubic nickel surface of the composite nanofibers became rougher after the carbonization process, and the diameters decreased from about 200 to 150 nm. The presence of Ni nanoparticles could also be further observed from the transmission electron microscope (TEM) image, as illustrated in *Fig. 2(c)*. Cubic nickel particles with diameters of 20-70 nm were well-dispersed along porous carbon nanofibers. Such a result suggested that the physical size of particle looked larger than the size calculated by Debye-Scherrer formula. This was because the particles measured by TEM contained several primary crystallite grains leading to a larger TEM particle size than that of measured by XRD [19].

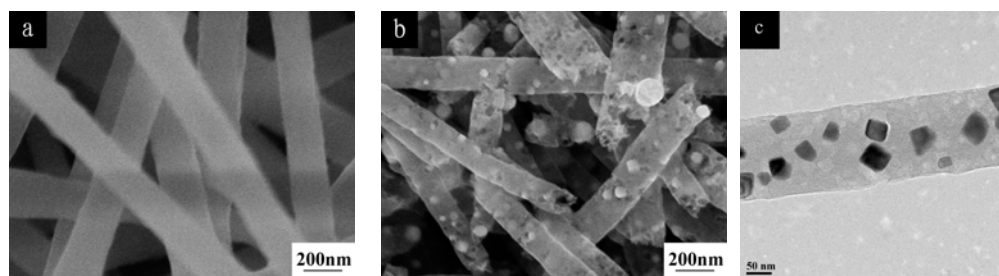


FIGURE 2. SEM images (mag.: ×50k) of PAN/PVP/Ni(OAc)<sub>2</sub> precursor (a), carbonized composite nanofibers (b), and TEM image of carbonized composite nanofibers (c).

### **Surface Area and Conductivity**

The nitrogen adsorption-desorption isotherms and pore size distribution curves of C/Ni composite nanofibers are shown in *Figure 3*. It exhibits type IV isotherms with type H4 hysteresis loops according to IUPAC classification [20], which are typical characteristics of mesoporous materials. The microporosity and mesoporosity were 28.1% and 41.4%, respectively. The pores were mainly produced by decomposition of PVP during carbonization. The BET surface area of C/Ni composite nanofibers was 28.6 m<sup>2</sup>/g, much larger than that of pure PAN carbon nanofibers(2.7m<sup>2</sup>/g). The direct current electrical

conductivity of the carbonized PAN and PAN/PVP/Ni(OAc)<sub>2</sub> fiber mats was determined by four probe conductivity method. The electrical conductivity of carbon fiber and carbon fiber containing different amount of nickel (6.5wt, 16.6wt% and 23.7wt%) fibers were 1.27, 2.0, 2.62 and 3.75 S/m, respectively, which was about a factor of three higher than the lower. So C/Ni composite fiber mats can be directly used as electrodes in supercapacitor without adding any polymer binder and conductive material.

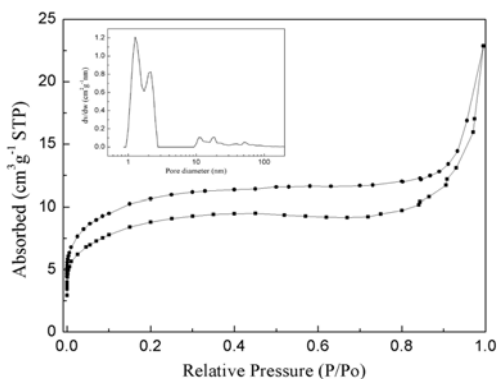


FIGURE 3. Nitrogen adsorption-desorption isotherms and pore size distribution curves of C/Ni composite nanofibers.

### Electrochemical Performance

Figure 4 presents typical potential-time curves of the samples in a 6 mol/L KOH solution at current density from 0.5 to 25 A/g obtained during galvanostatic charge/discharge for the cells. The curve in the potential range is approximately linear, which shows the absence of faradaic reactions and the discharge time decreased with increasing current.

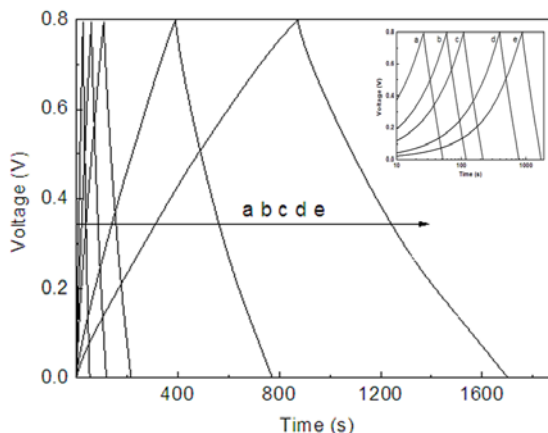


FIGURE 4. Charge-discharge behavior at different current densities (A/g). (a) 0.5, (b) 2.5, (c) 5.0, (d) 15.0, (e) 25.0.

The typical cyclic voltammograms (CVs) of carbon fibers with Ni composite electrode are shown in Figure 5 (a). In our case, all the CVs curves show no peaks, indicating that the composite electrodes had satisfactory electrochemical behavior in the electrochemical capacitors, even at high scan rate. However, deviation from the ideal rectangular shape at about 0.1 V could be attributed to the presence of surface functional groups making a pseudo-capacitance contribution [21]. Because the introduction of Ni imparted a surface polarity to the carbon surface, Faradaic reaction could occur in the region near the current collector in the surface of the carbon.

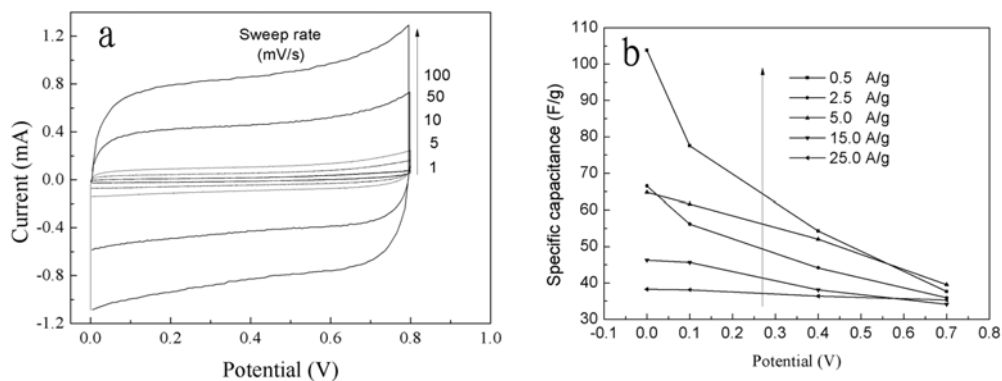


FIGURE 5. CVs of composite electrodes at different scan rate (a) and the specific capacitance as a function of voltage at different current densities (b).

The charge/discharge between 0 and 0.8 V was employed to estimate the capacitance of the electrodes in the cells, which is shown in Figure 5(b). The results showed that the capacitance decreased from 103.8 F/g to 38.25 F/g with increasing current density from 0.5

A/g to 25.0 A/g, while the power density increased from 102.7 W/kg to 4528.0 W/kg. The specific capacitance of the electrode was up to 47.2 F/g at 5.0 F/g with 73.8% of its initial value. Although the surface polarity and increased surface area could improve the

wettability of carbon and make it more accessible to electrolyte, it would still need enough time to access the porous structure of the electrode [15]. That was believed to be why the specific capacitance was much higher at low current density.

## CONCLUSIONS

In summary, porous C/Ni composite nanofibers with large specific surface area were successfully fabricated by combination of electrospinning and subsequent carbonization processes. The composite nanofibers consisted of FCC crystal structures and showed a high discharge capacity of 103.8 F/g, which 73.8% of the initial capacity remained after 100 charge/discharge cycles at 5.0 F/g. This approach is further applicable to different organic/inorganic composite nanofibers and opens up new avenues to the rational design of electrochemical materials with organic/inorganic architectures, such as C/Co, C/Cu or C/Mn composite nanofibers.

## ACKNOWLEDGEMENTS

The work was financially supported by the National High-tech R&D Program of China (No.2012AA030313), Changjiang Scholars and Innovative Research Team in University (No.IRT1135), National Natural Science Foundation of China (No.51006046 and No.51163014), the Priority Academic Program Development of Jiangsu Higher Education Institutions, Key Laboratory for Advanced Technology in Environmental Protection of Jiangsu Province (AE201321).

## REFERENCES

- [1] Niu HT, Zhang ZL, Wang X.. Carbon 2011; 49: 2380-2388.
- [2] Goswami S, Maiti UN, Maiti S, Nandy S, Mitra MK. Carbon 2011; 49: 2245-2252.
- [3] Liao HH, Qi RL, Shen MW, Cao XY, Guo R. Coll. and Surf. B: Biointerfaces 2011; 84: 528-535.
- [4] Cai YB, Gao DW, Wei QF, Gu HL, Zhou S, Huang FL, Song L, Hu Y, Gao WD. Fiber Polym. 2011; 12: 145-150.
- [5] Wei L, Adanur S. Text. Res. J. 2010; 80:124-134.
- [6] Suarez-Garcia F, Vilaplana-Ortego E, Kunowsky M, Kimura M, Oya A. Int. J. Hydrogen Energy 2009; 34: 9141-9150.
- [7] Kang SC, Im JS, Lee SH, Bae TS, Lee YS. Collid. Surface A 2011; 384: 297-303.
- [8] Oh GY, Ju YW, Jung HR, Lee WJ. J. Anal. Appl. Pyrolysis 2008; 81: 211-217.
- [9] Chan K, Kap-Seung Y, Lee WJ. Electrochem. Solid St. 2004; 7: 397-399.
- [10] Tavanai H, Jalili R, Morshed M. Surf. Interface Anal 2009; 41: 814-819.
- [11] Kim HY, Lee DH, Moon JH. J. Hydrogen Energy 2011; 36: 3566-3573.
- [12] Dhanabalan A, Yu Y, Li XF, Bechtold K, Maier J, Wang CL. Micro- and Nanotechnology Sensors, Systems, and Applications II 2010; 7679: 7679211-7679217.
- [13] Rajzer I, Rom M, Blazewicz M. Fiber Polym. 2010, 11: 615-624.
- [14] Qi RL, Guo R, Shen MW, Cao XY, Zhang LQ, Xu JJ, Yu JY, Shi XY. J. Mater. Chem. 2010; 20:10622-10629.
- [15] Li J, Liu EH, Li W, Meng XY, Tan ST. J. Alloy Compd. 2009; 478: 371-374.
- [16] Bellan LM, Craighead HG. Polym. Advan. Technol. 2011; 22: 304-309.
- [17] Gao DW, Qiao H, Wang QQ, Cai YB, Wei QF. J. Eng. Fiber Fabr. 2011; 6: 6-9.
- [18] Xu B, Zhang H, Cao GP, Zhang WF, Yang YS. Prog. Chem. 2011; 23: 605-611.
- [19] Hyde T. Platinum Met Rev 2008; 52: 29-130.
- [20] Sing KSW, Everett DH, Haul RAW, Moscou L, Pierotti RA, Rouquerol J, Siemieniewska T. Pure Appl. Chem. 1985; 57:603-619.
- [21] Jagannathan S, Chae HG, Jain R, Kumar S. J. Power Sources 2008; 185: 676-684.

**AUTHORS' ADDRESSES**

**Dawei Gao**

**Lili Wang**

College of Textiles and Clothing  
Yangcheng Institute of Technology, Yangcheng,  
Jiangsu  
CHINA

**Xin Xia**

**Hui Qiao**

**Yibing Cai**

**Fenglin Huang**

**Qufu Wei**

Key Laboratory of Eco-textiles,  
Ministry of Education,  
Jiangnan University,  
Wuxi, Jiangsu,  
CHINA

**Kishor Gupta**

**Satish Kumar**

School of Materials Science and Engineering  
Georgia Institute of Technology  
Atlanta, GA 30332  
UNITED STATES